Full Wave Numerical Simulation of a Finite 3D Metamaterial Lens

Ali Eren Culhaoglu[1], Michael Zedler[2], Wolfgang J. R. Hoefer[3], Andrey Osipov[1] and Peter Russer[2]

[1] Microwaves and Radar Institute,
German Aerospace Center, 82234 Wessling Germany
Ali.Culhaoglu@dlr.de, Andrey.Osipov@dlr.de

[2] Lehrstuhl fuer Hochfrequenztechnik
Technische Universitaet Muenchen, Arcisstrasse 21, 80333 Munich Germany
michael.zedler@tum.de, russer@tum.de

[3] Department of Electrical and Computer Engineering
University of Victoria, P.O. Box 3055 STN CSC Victoria, B.C. V8W 3P6 Canada
whoefer@ECE.Uvic.CA

Abstract: The concept of the double negative (DNG) perfect lens made of left handed material having negative permittivity and permeability has attracted growing interest. With the realization of such a lens the diffraction limit was overcome and sub-wavelength imaging became possible. However it has to be considered that the imaging quality is limited by the transverse extension of the Pendry lens. In this work we investigate the influence of the aperture of the Pendry lens on the imaging qualities. A full wave numerical analysis of a three-dimensional, finite-sized and impedance matched DNG slab is performed.

Keywords: Metamaterial, Double negative slab, Perfect lens, Imaging quality and 3D full wave simulation

1. Introduction

In 1968 Veselago first discussed the propagation of electromagnetic waves in materials having simultaneously negative permittivity and permeability [1]. He showed that waves propagating in such media are backward waves exhibiting negative phase velocity and also negative refractive index. Three decades later Pendry [2] demonstrated the possibility of sub-wavelength imaging with a double negative (DNG) flat slab made of such materials and showed that it is possible to realize high resolution lenses that can resolve details finer than the wavelength. However DNG materials do not occur in nature. A composite medium first has been realized by the group of Smith [3], [4] in which both the effective permittivity and permeability showed negative values over a finite frequency band. Up to now only flat Pendry lenses in two dimensions have been investigated. In this paper three dimensional simulations of finite slabs are presented. Since a physical realization of this simulation setup requires fully 3D metamaterials, one of the following topologies could be

used: A FDTD-derived structure independently proposed in [5] and [6], a structure derived from the rotated transmission line matrix (TLM) scheme [7], a structure consisting of dielectric spheres [8], a 3D extension of the wire/ split-ring approach [9], [10] and a straightforward extension of the 1D/ 2D composite right-left-handed (CRLH) structure [11], [12], which was the first 3D DNG metamaterial demonstrated experimentally. For finite-sized slabs physical phenomena like edge diffraction can negatively affect the focusing quality. Therefore the influence of the transverse extension of the DNG slab onto its focusing properties is investigated. In this work the simulations are carried out with MEFISTo-3D Pro [13], a full wave time domain electromagnetic simulation tool, based on the TLM method.

2. Theory and Numerical Simulations

A. Theory

Veselago pointed out that a slab with two parallel plane surfaces having negative refractive index would collect a wave originating from a point source on the one side of the slab into a focal point at the other side and therefore act as a collimating lens [1].
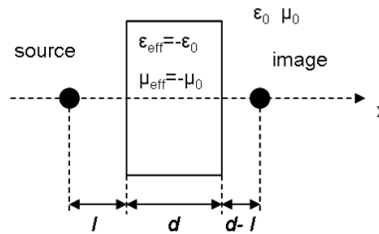

Fig. 1. DNG slab acting as a lens.

As shown in Fig. 1, light transmitted through a slab of thickness d located at a distance l from the source is focused at a plane located at

$$x = d - l, \tag{1}$$

with respect to the right surface of the slab. According to the definition of the refractive index

$$n = \sqrt{\epsilon_r \mu_r}, \tag{2}$$

a negative relative permittivity and relative permeability of the DNG medium imply a negative n. This results from the fact that the negative value of the square root has to be chosen when both ϵ_r and μ_r are negative [1]. On the other hand the impedance of the medium

$$Z = \sqrt{\frac{\mu_r \mu_0}{\epsilon_r \epsilon_0}} = \sqrt{\frac{\mu_r}{\epsilon_r}} Z_0, \ with \ Z_0 = \sqrt{\frac{\mu_0}{\epsilon_0}}, \tag{3}$$

remains positive. Choosing $\epsilon_r = -1$ and $\mu_r = -1$ yields a metamaterial with characteristic impedance equal to the characteristic impedance of free space. We note that real metamaterials are strongly dispersive and the required refractive index and wave impedance values usually can be realized only within a narrow frequency band.

B. Simulation Space

We consider a lossless DNG medium matched to free space at 10 *GHz*. The DNG slab has a thickness of 60 *mm*, which equals 2 λ. The configuration is excited with a vertical electric dipole that is placed 30 *mm* in front of the slab. The simulation volume has dimensions of 800x300x300 *mm* and is discretized with a 3 *mm* general symmetrical condensed node (GSCN) mesh. The optical axis of the device is along the *x*-axis. All simulations have been truncated after 1020 time steps, when a steady state is reached. Due to symmetry we can impose electric and magnetic walls on the *xy* and *xz*-planes, respectively. This makes it possible to restrict our simulations to a single quadrant of the DNG slab as shown in Fig. 2. All other boundaries are absorbing. The DNG slab is surrounded by an absorber of the same thickness.
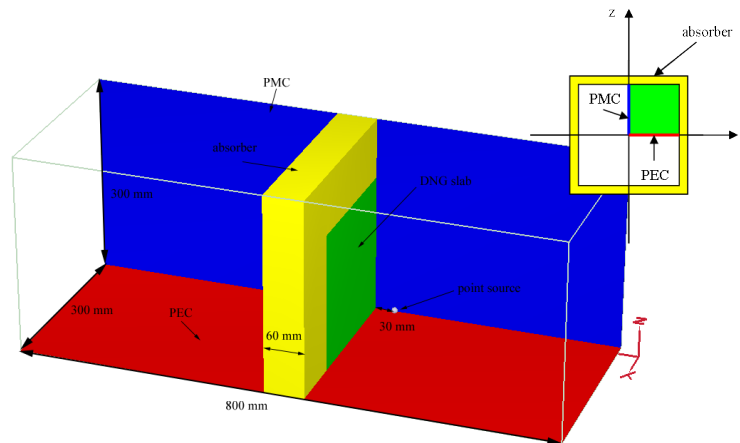
Fig. 2. The simulation volume.

C. Numerical Simulations

According to (1) the image of the point source is expected to be at a distance of 30 *mm* from the rear side of the slab. To evaluate the electric field intensity a plane of reference is positioned there. Throughout the simulations the lateral extension of the slab is varied from 1 to 20 λ and the intensity distribution of the electric field on the screen is observed (Fig. 3).
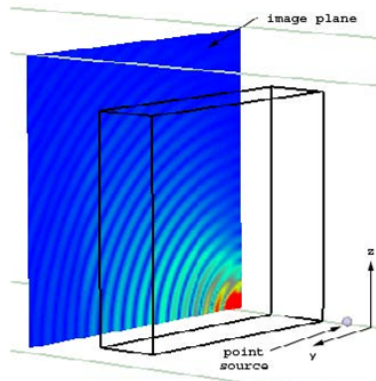
Fig. 3. Electric field intensity distribution on a plane positioned at the expected image location ($t = 1020\Delta t$ for a slab size of 16 λ).

Some of the simulation results are given in Fig. 4. The left and right figures show the electric field intensity distribution for slabs with a lateral extension of 2 and 16 λ, respectively. Two figures confirm that the imaging quality enhances with increasing slab size. In the figure on the right the first image at the internal of the slab and the second image behind the slab are clearly visible. In the following section we analyze the focusing performance of the slab for different apertures and give a relationship between the aperture size and the focusing quality. For this purpose the mean and standard deviations of the intensity distribution along the plane of reference are calculated.
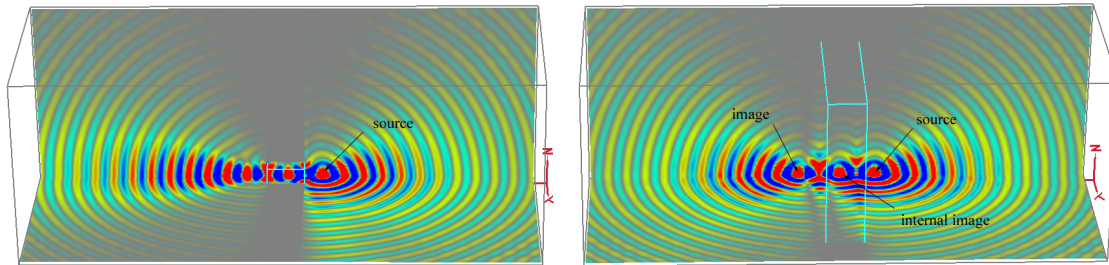

Fig. 4. Electric field intensity at $t = 1020\Delta t$, for a 2 λ slab on the left and a 16 λ slab on the right.

3. Results

The lateral extension of the aperture is varied between 1-20 λ (30-600 mm). In Fig. 5 a plot of the instantaneous intensity distribution at $t = 1020\Delta t$ along the optical axis for various slab sizes is shown. It is noticed that the intensity at the image plane increases with increasing slab dimensions. Furthermore, if we take a look at the intensity distribution along the plane of reference (Fig. 6) it can be concluded that for a slab with a lateral extension of 1 λ there is no focusing at all. By increasing the aperture size the peak intensity changes significantly. A further increase (approximately from 6 λ upwards), however, results only in a slight enhancement. This can also be concluded from Fig. 5, where the intensity distributions for 8, 14 and 20 λ are almost identical and overlap. In Fig. 7 the imaging quality as a function of the lateral extension of the slab is plotted. For each slab its imaging quality has been calculated as the standard deviation or lateral spread from the mean intensity along the plane of reference. As expected, the focus quality increases monotonically. For small lateral extensions (1-4 λ) we observe a radical improvement in the focusing quality. For larger slab sizes the curve becomes smoother and the improvement in the focusing quality slower.

4. Conclusion

A numerical analysis of the impact of the lateral extension of a 3D DNG slab onto its focusing quality has been given. The lateral extent of the slab was varied from 1 to 20 λ. The standard deviation of the intensity distribution along a reference plane positioned at the focal point has been used as a measure for the imaging quality. As expected from theory, the focusing behavior of the slab increases with increasing lateral extension. It can be concluded that for slabs with a lateral extension smaller than 5 λ, focusing quality improves significantly with increasing size. In future work the influence of the position of the source and thickness of the slab onto its focusing quality will be investigated.
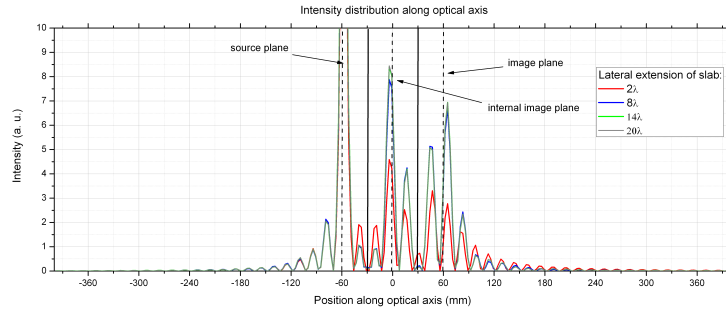
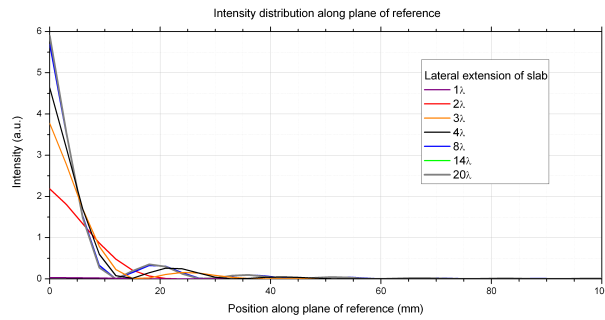Fig. 5. Intensity distribution at $t = 1020\Delta t$ along optical axis for different slab sizes.

Fig. 6. Intensity at the plane of reference at $t = 1020\Delta t$ for various lateral extensions of the slab.
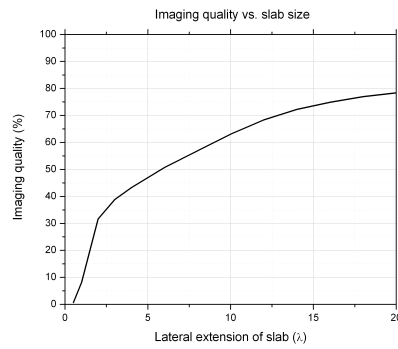
Fig. 7. Focal quality vs. slab size.

References

[1] V. G. Veselago, "The Electrodynamics of Substances with Simultaneously Negative Values of ϵ and μ," *Sov. Phys. Uspekhi*, Vol. 10, pp. 509, 1968.

[2] J. B. Pendry, "Negative Refraction Makes a Perfect Lens," *Physical Review Letters*, Vol. 85, pp. 3966, 2000.

[3] D. R. Smith, W. Padilla, D. Vier, S. Nemat-Nasser and S. Schultz, "Composite medium with simultaneously negative permeability and permittivity," *Physical Review Letters*, Vol. 84, pp. 4184, 2000.

[4] R. A. Shelby, D. R. Smith and S. Shultz, "Experimental verification of a negative index of refraction," *Science*, Vol. 292, pp. 77, 2001.

[5] W. Hoefer, P. So, D. Thompson and M. Tenzeris, "Topology and Design of Wide-Band 3D Metamaterials made of Periodically Loaded Transmission Lines," *2005 Int. Microwave Symposium Digest, Long Beach*, pp. 1443, 2005.

[6] A. Grbic and G.V. Eleftheriades, "An isotropic three-dimensional negative-refractive-index transmission line metamaterial," *J. Appl. Physics*, Vol. 98, 2005.

[7] M. Zedler, C. Caloz and P. Russer, "A 3D Isotropic Left-Handed Metamaterial based on the Rotated Transmission Line Matrix (TLM) Scheme," *Transactions on Microwave Theory and Techniques, IMS Special Issue*, Accepted for publication, 2007.

[8] I. Vendik, O. Vendik and M. Odit, "Isotropic Artificial Media with Simultaneously Negative Permittivity and Permeability," *Microwave and Optical Technology Letters*, Vol. 48, 2006.

[9] P. Kip Mercure, Robert P. Haley, Andrew Bogle and Leo Kempel, "Three-dimensional Isotropic Meta-materials," *2005 Int. Antennas and Propagation Society Symposium Digest*, pp. 623, 2005.

[10] Th. Koschny, L. Zhang and C.M. Soukoulis, "Isotropic three-dimensional left-handed meta-materials," *Physical Review B*, Vol. 71, pp. 121103, 2005.

[11] Pekka Alitalo, Stanislav Maslovski and Sergei Tretyakov, "Three-dimensional isotropic perfect lens based on LC-loaded transmission lines," *J. Appl. Physics*, Vol. 99, 2006.

[12] Pekka Alitalo, Stanislav Maslovski and Sergei Tretyakov, "Experimental verification of the key properties of a three-dimensional isotropic transmission-line superlens," *J. Appl. Physics*, Vol. 99, 2006.

[13] MEFiSTo-3D Pro, version 5.0, *Faustus Scientific Corporation*, 1256 Beach Drive, Victoria, BC, V8S 2N3, Canada.